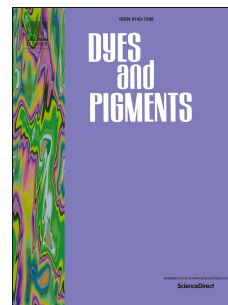# Accepted Manuscript

Comparative photodynamic inactivation of bioluminescent *E. coli* by pyridinium and inverted pyridinium chlorins

Joana M.D. Calmeiro, Cristina J. Dias, Catarina I.V. Ramos, Adelaide Almeida, João P.C. Tomé, Maria A.F. Faustino, Leandro M.O. Lourenço

Please cite this article as: Calmeiro JMD, Dias CJ, Ramos CIV, Almeida A, Tomé JoãPC, Faustino MAF, Lourenço LMO, Comparative photodynamic inactivation of bioluminescent *E. coli* by pyridinium and inverted pyridinium chlorins, *Dyes and Pigments* (2019), doi: https://doi.org/10.1016/j.dyepig.2019.03.021.

This is a PDF file of an unedited manuscript that has been accepted for publication. As a service to our customers we are providing this early version of the manuscript. The manuscript will undergo copyediting, typesetting, and review of the resulting proof before it is published in its final form. Please note that during the production process errors may be discovered which could affect the content, and all legal disclaimers that apply to the journal pertain.

R = ·⅟·S⟨ ⟩N⁺— or ·⅟·N⁺⟨ ⟩O
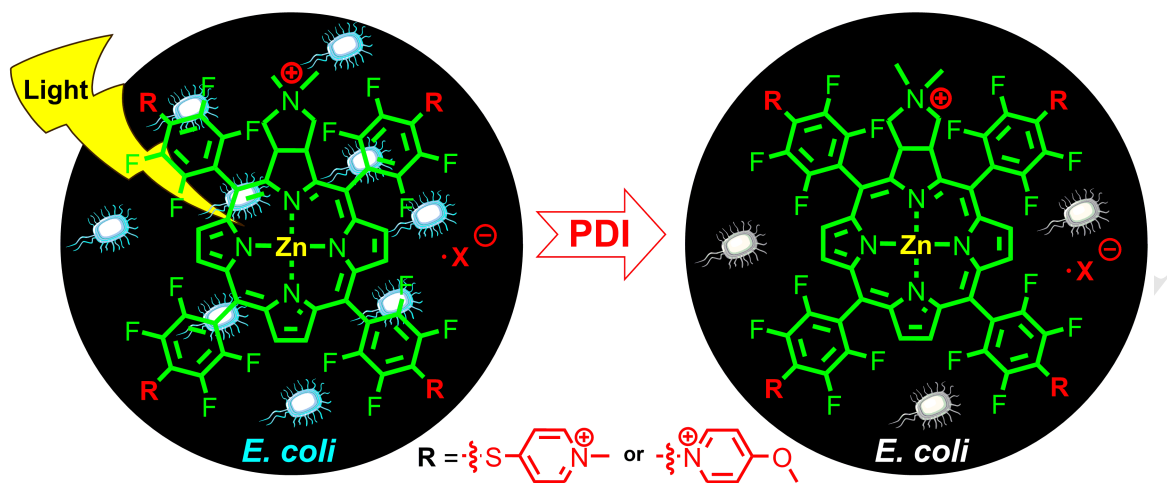
1 **Comparative photodynamic inactivation of bioluminescent *E. coli* by pyridinium and inverted**

2 **pyridinium chlorins**

3 Joana M. D. Calmeiro,[a] Cristina J. Dias,[b] Catarina I. V. Ramos,[a] Adelaide Almeida,[b] João P. C.

4 Tomé,[c] Maria A. F. Faustino,[a,*] Leandro M. O. Lourenço[a,*]

5 *[a]QOPNA & LAQV-REQUINTE and Department of Chemistry, University of Aveiro, 3810-193*

6 *Aveiro, Portugal*

7 *[b]CESAM and Department of Biology, University of Aveiro, 3810-193 Aveiro, Portugal*

8 *[c]CQE and Departamento de Engenharia Química, Instituto Superior Técnico, Universidade de*

9 *Lisboa, 1049-001 Lisboa, Portugal*

10 *E-mail: faustino@ua.pt; leandrolourenco@ua.pt

11

Abstract

13 Photodynamic inactivation (PDI) is a therapeutic approach in study due to the ability to reduce or

14 completely eliminate the bacterial strains without the development of resistance mechanisms. In this

15 therapeutic methodology the cationic chlorins (Chls) with pyridinium or inverted pyridinium moieties

16 are one of the photosensitizers exploited in our biological approaches. In this context, we synthesized

17 and characterized new free-base and zinc(II) complexes of pyridinium or inverted pyridinium Chl

18 derivatives (**1b**, **2**, **2a** and **2b**, respectively) for the inactivation of *Escherichia coli* (*E. coli*). The PDI

19 assay was performed with white light irradiation delivered at a fluence rate of 25 mW.cm^{-2}. The

20 obtained results of this study demonstrate high PDI efficiency of the zinc(II) metallated Chl **1b**,

21 reaching the detection limit of the bioluminescent method (5.2 log reduction) in 45 min of irradiation.

22

Introduction

24 As human population increases, the demand for basic goods and the removal of harmful

25 microorganisms, such as bacteria, viruses and protozoa, assumes greater worldwide significance and

26 becomes more difficult. Although the transmission of microbial diseases has been reduced by the

27 development of water supplies and hygienic procedures for a whole range of human activities [1–3],

28 the antimicrobial resistance has become a global threat to human health as a consequence of the

29 excessive and inappropriate use of antibiotics. The ability of the bacteria to develop mutations that

30 help their survival in the presence of antibiotics is responsible for the increasing number of resistant

31 bacteria strains that will quickly become predominant in the microbial population [4–8]. The

32 resistance development by the bacteria facing the conventional antibiotics have led the scientific

33 community to increase efforts to find alternatives against to this emergent resistance [9–12].

34 In this context, the antimicrobial photodynamic therapy (aPDT) or photodynamic inactivation (PDI)

35 has been considered an efficient and non-toxic therapeutic approach for the photoinactivation of

36 microorganisms to treat microbial infections and has been recognized as an alternative to the

37 conventional treatments (*e.g.* antibiotics) [13–16]. This therapeutic approach has evidenced the

38 ability to reduce or completely eliminate the bacterial strains without the development of resistance

39 mechanisms due to the numerous biochemical targets [6,17–21]. The action mode is based in

40 photodynamic action that has also been used in cancer photodynamic therapy (PDT) [22–24],

41 wastewater treatment [25–27], among others [28,29]. In the photodynamic approach it is used three

42 non-toxic elements: a photosensitizer molecule (PS), appropriate light (visible) and molecular oxygen

43 ($^3O_2$), that when combined generate highly reactive oxygen species (ROS), such as singlet oxygen

44 ($^1O_2$) and free radicals, which can induce lethal oxidative damage in the pathogenic microbial agents

45 (*e.g.* bacteria, viruses, fungi and protozoa) [9,15,30–32].

46 The identification of new promising PSs that can kill the microorganisms rapidly and efficiently has

47 been under investigation in order to identify more efficient PSs and to establish structure-activity

48 relationship. Several photosensitizer molecules, such as porphyrins (Pors) [33–41], chlorins (Chls)

49 [18,42–46] and phthalocyanines (Pcs) [47–53] are promising PS candidates for the photoinactivation

50 of microorganisms upon light activation at micromolar concentrations.

51 In particular, the Chl derivatives have been exploited as one of the most interesting photoactive

52 compounds, due to their high absorption in the visible region of the electromagnetic spectrum (350 -

800 nm). They present a Soret band maximum ~ 400 nm (blue region) and an intense Q-band between 650 - 670 nm (red region) [43,54–57]. Since Chl derivatives have two predominant absorption areas, they can be used to photoinactivate microorganisms in the clinic, industrial or environment scenarios, under different lights [58–61].
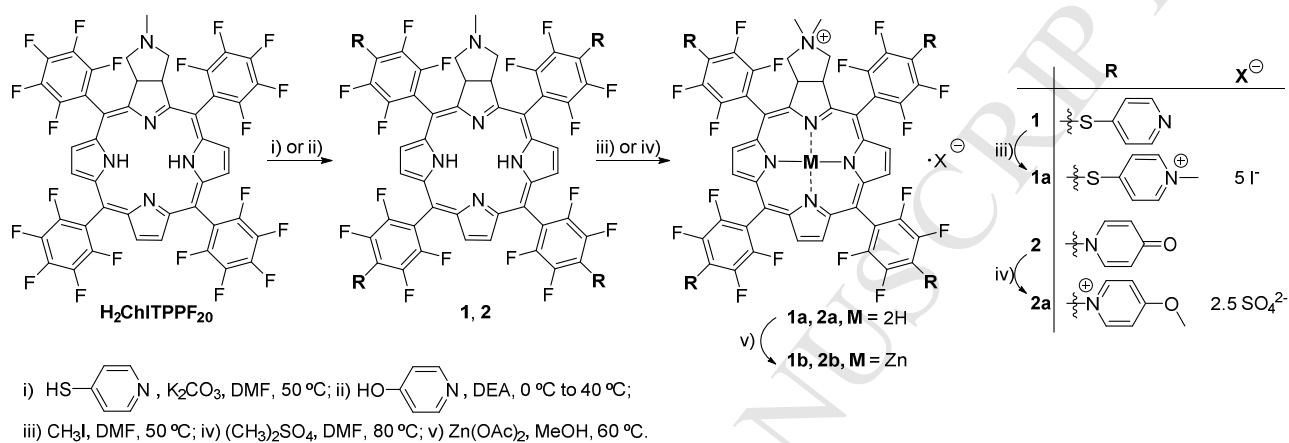
Since the chemical structure is a key factor in the PS physicochemical and biological properties, different approaches have been used to introduce specific functionalities on the Chl core [28]. The tetrapyrrolic core of the Chl template can be post-modified by incorporation of peripheral substituents [43,62], or by core metalation with different metal ions (*e.g.* Zn(II), Al(II), Pd(II), Pt(II)) [63,64], that can result in an enhancement of the triplet excited state parameters (triplet quantum yield and lifetime) and $^1O_2$ quantum yield [64,65]. These adjustments can unequivocally modulate the photophysical and photochemical features of Chl derivatives and affect their interaction with microbial cells, triggering different photobiological effects.

A well stablished structure-activity relationship between the PS features and the type of bacteria is that Gram-positive bacteria are efficiently photoinactivated by a variety of PSs, whereas Gram-negative bacteria are usually (photo)resistant to the action of neutral and anionic PSs [66–68]. However, cationic PSs, namely porphyrins and their Chl analogues have been shown to efficiently photoinactivate Gram-negative bacteria [18,68,69]. In fact, molecules positively charged can promote electrostatic interactions with the negative charge of the outer membrane of Gram-negative bacteria. This binding interaction PS-bacterium is essential to promote the PS contact with the target microorganism and enhance the bacteria damage efficiency [9,70,71]. Another established relationship is the number and the position of the charges in the PS, that have a clear effect on the overall efficiency of the PDI process namely in the Gram-negative bacterium *Escherichia coli* (*E. coli*) [72–74].

Considering PDI as a particular therapeutic approach for the treatment of microbial infections [43] or contaminated media [58,75], this work aims to study the inactivation efficiency of new PSs, and establish the relationships between the Chl core of a free-base thiopyridinium **1a** [18], the new inverted methoxypyridinium **1b** and their corresponding zinc(II) derivatives **2a** and **2b** (Scheme 1).

3

80 These cationic Chls were prepared from the fluorinated Chl, obtained from 5,10,15,20-

81 tetrakis(pentafluorophenyl)porphyrin **TPPF$_{20}$** [18]. The photophysical properties and the ability of

82 the new water soluble Chl derivatives **1b**, **2a** and **2b** to photoinactivate microorganisms under white

83 light irradiation (400 - 800 nm) was evaluated against a bioluminescent *E. coli* recombinant strain,

84 used as a model of Gram-negative pathogenic bacteria and compared with Chl **1a**.

85

i) HS—⬡—N , K$_2$CO$_3$, DMF, 50 ºC; ii) HO—⬡—N , DEA, 0 ºC to 40 ºC;

86 iii) CH$_3$I, DMF, 50 ºC; iv) (CH$_3$)$_2$SO$_4$, DMF, 80 ºC; v) Zn(OAc)$_2$, MeOH, 60 ºC.

87 **Scheme 1**

88

89 **Experimental**

90 **Photosensitizers synthesis and characterization**

91

92 The synthetic methodology for the preparation of the water soluble Chl quaternary salts with

93 different substituent groups (Chls **1a** and **2a**) and their metallated derivatives (Chls **1b** and

94 **2b**) is depicted in Scheme 1. Chlorins identified as **H$_2$TPChlF$_{20}$, 1** and **1a** were synthetized

95 according to previously described procedures[18,33] and Chl derivatives **1b**, **2**, **2a** and **2b**

96 were prepared using adequate reagents purchased from Sigma-Aldrich. Analytical TLC was

97 carried out on pre-coated silica gel sheets (Merck, 60, 0.2 mm). Solvents were used as

98 received or distilled and dried by using standard procedures according to the literature [76].

99 ^{1}H and ^{19}F NMR spectra were recorded on a Bruker Avance-300 spectrometer at 300.13 and

100 282.38 MHz, respectively. Tetramethylsilane was used as internal reference. The chemical

4

101 shifts were expressed in δ (ppm) and the coupling constants (J) in Hertz (Hz). Absorption and

102 steady-state fluorescence spectra were recorded using a Shimadzu UV-2501PC and Horiba

103 Jobin-Yvon FluoroMax-3 spectrofluorometer, respectively. The absorbance and fluorescence

104 emission spectra of Chl derivatives **1a**,**b** and **2a**,**b** were measured in DMF in 1×1 cm quartz

105 optical cells at 298.15 K and under normal air conditions. The fluorescence quantum yield

106 (Φ_F) of **1a**,**b** and **2a**,**b** were calculated in DMF by comparison of the area below the corrected

107 emission spectra using **TPP** as standard ($\Phi_F = 0.11$ in DMF) [51]. The ESI mass spectra of

108 the compounds were obtained using Micromass Q-TOF2 equipment and the analysis were

109 recorded on Micromass MassLynx 4 data system.

110

111 ***N,N*-Dimethylpyrrolidinyl-5,10,15,20-tetrakis[2,3,5,6-tetrafluoro-4-(1-methylpyridinium-4-**

112 **ylsulfanyl)phenyl]chlorinato zinc(II)**, $ZnTPChlF_{16}SPy_4(CH_3)_4$ (**1b**): $H_2TPChlF_{16}SPy_4(CH_3)_4$ **1a**

113 [18] (60.0 mg, 0.040 mmol) and zinc(II) acetate (14.8 mg, 0.082 mmol) were left stirring overnight in

114 10 mL MeOH at 60 ℃ (Scheme 1). The green solution was concentrated and the product precipitated

115 in a mixture of $MeOH:CH_2Cl_2:Acetone$ (5:2:1). The compound was obtained as a dark green powder

116 and was identified as **1b** (44.3 mg, 0.028 mmol), 71% of yield. ^{1}H NMR (300.13 MHz, DMSO-d_6): δ

117 2.28 (*dt*, $J = 3.6$, 1.7 Hz, 2H, pyrrolidine-H), 2.73 (*dt*, $J = 3.6$, 1.7 Hz, 2H, pyrrolidine-H), 3.27 (*s*,

118 6H, $-N(CH_3)_2$), 4.32 (*s*, 12H, Py-NCH$_3$), 5.76-5.85 (*m*, 2H, β-H reduced pyrrole), 8.29-8.34 (*m*, 2H,

119 β-H pyrrole), 8.35-8.50 (*m*, 8H, Py-*o*-H), 8.77-8.83 (*m*, 2H, β-H pyrrole), 8.89-8.96 (*m*, 8H, Py-*m*-H),

120 9.00-9.07 (*m*, 2H, β-H pyrrole). ^{19}F NMR (282.38 MHz, DMSO-d_6): δ -163.40 to -162.42 (*m*, 2F, Ar-

121 F), -160.31 to -160.09 (*m*, 4F, Ar-F), -158.09 to -157.38 (*m*, 2F, Ar-F), -155.88 to -155.66 (*m*, 4F, Ar-

122 F), -153.98 to -152.68 (*m*, 4F, Ar-F). UV-Vis (DMF), λ_{max} (log ε): 416 (5.26), 515 (3.92), 585 (3.98),

123 618 (4.56) nm. **ESI-MS** (*m/z*): 510.8 $[M^{5+}+2e^-]^{3+}$, 479.8 $[M^{5+}+e^--C_6H_7N]^{3+}$, 469.1 $[M^{5+}+e^-$-

124 $C_6H_7NS]^{3+}$, 438.2 $[M^{5+}-C_6H_7NS-C_6H_6N]^{3+}$, 673.1 $[M^{5+}-C_6H_7N-C_6H_6N]^{2+}$, 657.6 $[M^{5+}-C_6H_7NS-$

125 $C_6H_6N]^{2+}$, 649.6 $[M^{5+}-C_6H_7NS-C_6H_6N-CH_3]^{2+}$, 612.1 $[M^{5+}-C_6H_6NS-2C_6H_6N]^{2+}$, 596.1 $[M^{5+}$-

126 $2C_6H_6NS-C_6H_6N]^{2+}$.

127

129 **N-Methylpyrrolidinyl-5,10,15,20-tetrakis[2,3,5,6-tetrafluoro-4-(1,4-dihydro-4-**

130 **oxopyridin-1-yl)phenyl]-21,23H-chlorin**, $H_2TPChlF_{16}(NPyO)_4$ (**2**): A solution **A** of

131 **$H_2TPChlF_{20}$** (205.0 mg, 0.199 mmol) was prepared in 2.0 mL of DMF in a round-bottom

132 flask. At the same time, a solution **B** of 4-hydroxypyridine (77.0 mg, 0.796 mmol) and

133 diethylamine (DEA, 82.0 µL, 0.793 mmol) was prepared in 1.0 mL of DMF. Both solutions

134 were maintained stirring under N_2 atmosphere during 20 min at room temperature. Then, both

135 solutions were cooled (0 ºC) in an ice bath, and the solution **B** was dropwise added to solution

136 **A**. After 24 h of reaction at room temperature, the temperature was raised until 40 ºC and the

137 reaction carried out during another 24 h period. The reactional progression was controlled by

138 TLC. The crude was evaporated until complete dryness and the obtained green dark solid

139 crystalized from a mixture of MeOH:CH_2Cl_2:Hexane (2:3:1). A green dark powder was

140 obtained and identified as compound **2** (150.0 mg, 0.075 mmol), isolated in 57% of yield. ^{1}H

141 NMR (300.13 MHz, DMSO-d_6): δ -1.94 (s, 2H, -NH), 2.26-2.29 (m, 2H, pyrrolidine -NH),

142 2.43-2.45 (m, 3H, -NCH$_3$), 2.72-2.74 (m, 2H, pyrrolidine -NH), 5.44 – 5.63 (m, 2H, β-H

143 reduced pyrrole), 6.51-6.54 (m, 8H, NPyO-o-H), 7.95 (d, J = 6.8 Hz, 2H, β-H pyrrole), 8.14-

144 8.19 (m, 8H, NPyO-m-H), 8.98 (d, J = 5.1 Hz, 2H, β-H pyrrole), 9.30 (d, J = 5.1 Hz, 2H, β-H

145 pyrrole). ^{19}F NMR (282.38 MHz, DMSO-d_6): δ -172.27 (m, 4F, Ar-F), -170.39 to -171.22 (m,

146 4F, Ar-F), -162.29 (dt, J = 27.1, 10.7 Hz, 4F, Ar-F), -160.02 (d, 2F, Ar-F), -157.49 (s, 2F, Ar-

147 F). UV-Vis (DMF), λ_{max} (log ϵ): 406 (5.14), 503 (4.16), 527 (3.70), 595 (3.66), 648 (4.52)

148 nm. **ESI-MS** (m/z): 444.8 $[M+3H]^{3+}$, 666.7 $[M+2H]^{2+}$, 1332.54 $[M+H]^+$.

149

150

151 **N,N-Dimethylpyrrolidinyl-5,10,15,20-tetrakis[2,3,5,6-tetrafluoro-4-(4-**

152 **methoxypyridinium-1-yl)phenyl]-21,23H-chlorin**, $H_2TPChlF_{16}(NPyOCH_3)_4$ (**2a**):

153 $H_2TPChlF_{16}(NPyO)_4$ **2** (100.0 mg, 0.075 mmol) and dimethyl sulfate (71.0 µL, 0.751 mmol)

154 were dissolved in 5.0 mL of DMF and left to react overnight at 80 ºC in a sealed tube. The

reaction mixture was cooled and the compound was precipitated in diethyl ether. The obtained precipitate was filtered, washed with diethyl ether and dried under vacuum. The solid was dissolved in MeOH and reprecipitated in a mixture of MeOH:CH_2Cl_2 (1:2). The obtained green suspension was filtered, washed with CH_2Cl_2 and dried under vacuum. The obtained compound was identified as **2a** (33.0 mg, 0.021 mmol) isolated in 29% of yield. ^{1}H NMR (300.13 MHz, DMSO-d_6): δ -1.94 (*s*, 2H, -NH), 2.26-2.29 (*m*, 2H, pyrrolidine -NH), 2.42-2.45 (*m*, 6H, -N(CH_3)$_2$), 2.72-2.75 (*m*, 2H, pyrrolidine -NH), 4.36 (*s*, 6H, -NPyOCH_3), 4.37 (*s*, 6H, -NPyOCH_3), 5.95-6.06 (*m*, 2H, β-H reduced pyrrole), 8.18 (*m*, 8H, -NPyO-*o*-H), 8.97 (*s*, 2H, β-H pyrrole), 9.04 (*d*, *J* = 5.1 Hz, 2H, β-H pyrrole), 9.37 (*d*, *J* = 5.1 Hz, 2H, β-H pyrrole), 9.41-9.49 (m, 8H, -NPyO-*m*-H). ^{19}F NMR (282.38 MHz, DMSO-d_6): δ -170.78 (*dd*, *J* = 62.9, 24.7 Hz, 4F, Ar-F), -168.57 to -168.22 (*m*, 4F, Ar-F), -161.17 (*ddd*, *J* = 37.0, 25.7, 10.0 Hz, 4F, Ar-F), -159.83 (*dd*, *J* = 25.3, 9.1 Hz, 2F, Ar-F), -159.92 to -158.24 (*m*, 2F, Ar-F). UV-Vis (DMF), λ_{max} (log ε): 409 (4.95), 503 (3.53), 529 (3.58), 595 (4.19), 648 (3.55) nm. **ESI-MS** (*m/z*): 736.2 $[M^{5+}+SO_4^{2-}-OCH_3]^{2+}$, 704.2 $[M^{5+}+5e^-+2H]^{2+}$, 680.2 $[M^{5+}+H-3CH_3]^{2+}$, 673.7 $[M^{5+}+H-4CH_3]^{2+}$, 1471.7 $[M^{5+}+SO_4^{2-}-OCH_3]^+$, 1444.6 $[M^{5+}+SO_4^{2-}-C_3H_8N]^+$, 1407.6 $[M^{5+}+5e^-+H]^+$, 1346.5 $[M^{5+}-4CH_3]^+$.

***N*,*N*-Dimethylpyrrolidinyl-5,10,15,20-tetrakis[2,3,5,6-tetrafluoro-4-(4-methoxypyridinium-1-yl)phenyl]chlorinato zinc(II)**, ZnTPChlF$_{16}$(NPyOCH$_3$)$_4$ (**2b**): H$_2$TPChlF$_{16}$(NPyOCH$_3$)$_4$ **2a** (30.0 mg, 0.018 mmol) and zinc(II) acetate (3.5 mg, 0.036 mmol) were left stirring overnight in 6.0 mL of MeOH:CH_2Cl_2 at 60 ºC in a sealed tube. The reaction solution was concentrated and the obtained solid washed with acetone:hexane (1:1). The compound was filtered and dried under vacuum. The compound **2b** (22.2 mg, 0.014 mmol) was obtained in 80% of yield. ^{1}H NMR (300.13 MHz, DMSO-d_6): δ 2.26-2.28 (*m*, 2H, pyrrolidine-H), 2.43-2.45 (*m*, 6H, pyrrolidine-N(CH_3)$_2$), 2.71-2.74 (*m*, 2H, pyrrolidine-H), 4.35 (*s*, 12H, -NPyOCH_3), 5.83-5.97 (*m*, 2H, β-H reduced pyrrole), 8.16 (*d*, *J* = 7.1 Hz, 8H, -NPyO-*o*-H), 8.58 (*d*, *J* = 4.8 Hz, 2H, β-H pyrrole), 8.77 (*s*, 2H, β-H pyrrole), 8.94 (*d*, *J* = 4.8

182 Hz, 2H, β-H pyrrole), 9.44 (d, J = 6.2 Hz, 8H, -NPyO-m-H). ^{19}F NMR (282.38 MHz, DMSO-

183 d_6): δ -171.40 (d, J = 21.9 Hz, 4F, Ar-F), -169.22 (s, 4F, Ar-F), -161.56 to -161.06 (m, 4F, Ar-

184 F), -160.33 (s, 4F, Ar-F), -158.68 (s, 4F, Ar-F). UV-Vis (DMF), λ_{max} (log ε): 420 (5.30), 512

185 (4.18), 582 (3.82), 618 (4.58) nm. **ESI-MS** (m/z): 521.5 $[M^{5+}+SO_4^{2-}]^{3+}$, 489.5 $[M^{5+}+2e^-]^{3+}$,

186 484.2 $[M^{5+}+e^--CH_3]^{3+}$, 479.5 $[M^{5+}-2CH_3]^{3+}$, 726.7 $[M^{5+}+2e^--CH_3]^{2+}$, 718.7 $[M^{5+}-OCH_3]^{2+}$,

187 711.7 $[M^{5+}-3CH_3]^{2+}$, 687.2 $[M^{5+}-3OCH_3]^{2+}$.

188

189 **Photosensitizers stock solution**

190 Stock solutions of the photosensitizers (**1a**,**b** and **2a**,**b**) used in the photophysical studies were

191 prepared in DMF and for the biological studies in dimethyl sulfoxide (DMSO) at a concentration of

192 500 µM, protected from light, and were sonicated for 30 min previously each assay.

193

194 **Light source**

195 All the photodynamic inactivation assays were performed by exposing the samples and light controls

196 to a white light (400 - 800 nm) delivered from a compatible fiber optic probe attached to a 250 W

197 quartz/halogen lamp (LUMACARE model LC122, USA) with an irradiance of 25 mW.cm^{-2},

198 measured with an energy meter Coherent FieldMaxII-Top combined with a Coherent

199 PowerSensPS19Q energy sensor.

200

201 **Singlet oxygen generation**

202 The ability of the cationic Chls **1a**,**b** and **2a**,**b** to generate $^1O_2$ was evaluated by an indirect method

203 trough the monitorization of the photooxidation of 9,10-dimethylanthracene (9,10-DMA), a singlet

204 oxygen quencher [77,78]. The kinetics of 9,10-DMA photooxidation was studied by following the

205 decrease in the absorbance at 378 nm and the result registered in a first-order plot for the

206 photooxidation of 9,10-DMA in absence of a PS and photosensitized by **1a**,**b** and **2a**,**b** and **TPP** in

207 DMF. Solutions of cationic Chls derivatives and **TPP** in DMF with the same optical density were

8

208 irradiated in quartz cuvettes with monochromatic light in the presence of 9,10-DMA (30 μM). **TPP**

209 (in DMF) were used as reference (Φ_Δ = 0.65) [79]. The results are expressed as mean and standard

210 deviation obtained from three independent experiments. The singlet oxygen quantum yields (Φ_Δ)

211 were determined by the equation indicated below where Φ_Δ^{std} is the singlet oxygen quantum yield of

212 **TPP**, K_{sample} and K_{std} are the photodecay constant of 9,10-DMA in the presence of the sample and the

213 reference respectively, Abs_{sample} and Abs_{std} are the absorbance of the sample and the reference

214 solution at the irradiation wavelength.

$$\Phi_\Delta = \Phi_\Delta^{std} \frac{K_{sample}}{K_{std}} \frac{1 - 10^{-Abs_{std}}}{1 - 10^{-Abs_{sample}}}$$

215

Photostability

217 A solution of Chl derivatives **1a**,**b** and **2a**,**b** were freshly prepared in DMF and adjusted to an

218 absorbance ~ 1. The irradiation experiments were performed in magnetically stirred cuvette solutions

219 over a period of 120 min under the same light conditions used to perform the biological assays (400 -

220 800 nm, 25 mW.cm^{-2}). The absorbance of each solution was determined before (t = 0 min) and after

221 5, 15, 30, 60, 90, and 120 min of irradiation. The results were expressed as follows:

$$Photostability\ (\%) = \frac{Abs_{at\ a\ given\ time\ of\ irradiation}}{Abs_{t=0}} \times 100$$

222

Bacterial culture

224 Bioluminescent *E. coli* Top10 were grown on Tryptic Soy Broth (Liofilchem, Italy) medium at 25 ºC

225 for 18 h at 120 rpm in order to reach the stationary phase.

226 This bioluminescent *E. coli* strain was selected since the bacterial bioluminescence is a sensitive and

227 cost-effective method that allows a real-time monitoring, which gives a strong correlation between

228 bioluminescence signal and viable counts of the forming units, where the light output reflects the

229 actual cells´ metabolic rate [6,42,80].

9

Photodynamic inactivation assay

Bacterial suspensions were prepared from cultures ($\approx 10^8$-10^9 counting forming units (CFU.mL^{-1}) and several dilutions in PBS to a final concentration of $\approx 10^7$ CFU.mL^{-1}, and then distributed in sterilized glass beakers. The appropriate volume of each PS (**1a**,**b** and **2a**,**b**) was added to the suspensions to reach a final concentration of 5.0 µM. Light and dark controls were performed during the assay where, light control no PS was added and this was exposed to the white light and in the dark control PS was added in the same concentration (5.0 µM) and this was protected from light with aluminum foil. Samples were incubated under stirring for 15 min and protect from light. Following this period, the samples were irradiated under stirring during 120 min at a controlled temperature of 20 ºC. Aliquots of the treated and control samples were collected at time 0 min and after predefined irradiation times, and the bioluminescence was measured in triplicated in the luminometer (GloMax® 20/20 Luminometer, Promega, Madison, WI, USA). Three independent experiments were performed in duplicate.

Statistical analysis

Statistical analysis was performed in GraphPad Prism 6. The significance of the bacterial inactivation was assessed by two-way univariate analysis of variance (two-way ANOVA) model with the Turkey's multiple comparisons post hoc test. A value of $p < 0.05$ was considered significant.

Results and Discussion

Synthesis and photophysical characterization of the chlorin derivatives

The context of microbial resistance led to the search of new treatment modalities and consequently the research of new active principles in the PDI field and new efficient PSs. For that it is crucial to identify the structural features able to affect the PS efficiency. It is well-known that the presence of positive charges in the PS is an important feature but knowledge of how the accessibility of this

256 positives charge affects the photodynamic efficiency of the PS is still scarce [47,81]. Motivated by

257 this approach, this work is focused on synthesis of cationic Chls **1a,b** and **2a,b** to photoinactivate the

258 Gram-negative bioluminescent *E. coli* strain.

259

260 So, in order to obtain different positive charge accessibility, the new inverted pyridinone Chl **2**

261 present in Scheme 1 was prepared. Their synthesis was based on the nucleophilic substitution of the

262 *para*-fluorine atoms of **H₂TPChlF₂₀** with 4-hidroxypyridine, using DEA in DMF at room

263 temperature during 24 h and raised to 40 ºC during another period of 24 h. After the reaction work-

264 up, it was isolated in 57% of yield. The corresponding cationic Chl was obtained by methylation of **2**

265 with dimethyl sulfoxide in DMF at 80 ºC, being isolated in 29% of yield, mostly due to the difficult

266 removal of the dimethyl sulfate, used in excess. Both Chls **1b** and **2b** were obtained by direct

267 metalation with zinc(II) acetate in MeOH in 71% and 80% of yield, respectively. The structures of

268 **1b**, **2**, **2a**, and **2b** were confirmed by NMR (Figs. SI 2-9) and by mass spectrometry (Figs. SI 12-15),

269 as well as intermediate compounds **1** and **1a** (data not shown)[18]. Relative to the series of Chls **2**,

270 the substitution took place at the nitrogen and not at the oxygen as previously reported in the

271 substitution of Por [82]. When the cationization occurs, the carbonyl groups were converted into

272 methoxyls that generate a charge at the nitrogen atoms. The zinc(II) complexes were confirmed by

273 UV-Vis and the disappearance of the internal protons of the Chl core.

274 The ^{1}H NMR spectra of Chls **1b** and **2a,b** show the resonance of the characteristic signals of the

275 complete methylation of the pyridine moieties, specifically for the 12 protons of the pyridinium (Py-

276 NCH₃) and methoxypyridinium (-NPyOCH₃) groups around δ 4.32-4.37 ppm (Figures SI 2, SI 6 and

277 SI 8), respectively. Moreover, the complete Zn(II) metalation of Chls **1b** and **2b** was also confirmed

278 by the disappearance of the resonance signal corresponding to the internal NH protons of the free-

279 based Chls **1a** and **2a** at high fields (~ -2 ppm), respectively. The ^{19}F NMR spectra of all Chls (**1b**

280 and **2a,b**) show the resonance of five multiples corresponding to the fluorine atoms due to their

281 asymmetric distribution on the chlorin structure (Figures SI 3, SI 7 and SI 9).

282   In the ESI-MS spectra of the Chl derivatives **1b**, **2a** and **2b**, the main observed species result from

283   reduction processes with formation of ions with low overall *m/z* ratios, such as $[M^{5+}+2e^-]^{3+}$, $[M^{5+}+5e^-$

284    $+2H]^{2+}$ and $[M^{5+}+5e^-+H]^+$. These type of reduction processes were previously observed by us for

285   porphyrins [83,84]. Along with these ions, adduct formation with sulfate counter-ion $[M^{5+}+SO_4^{2-}]^{3+}$

286   were also observed, as well as ions resulting from losses of methyl, methylpyridinium or elements of

287   the methoxypyridinium substituents.

288   The absorption and emission spectra of Chls **1a**,**b** and **2a**,**b** were recorded in DMF solutions (~10^{-5}

289   M) at 298 K. All the main photophysical features such as Soret and Q band wavelengths, molar

290   extinction coefficients (ε), fluorescence emission wavelengths (λ_{emiss}), Stokes shift and fluorescence

291   quantum yields (Φ_F) are summarised in Table 1, and the absorption and emission spectra in DMF are

292   shown in Figure 1.
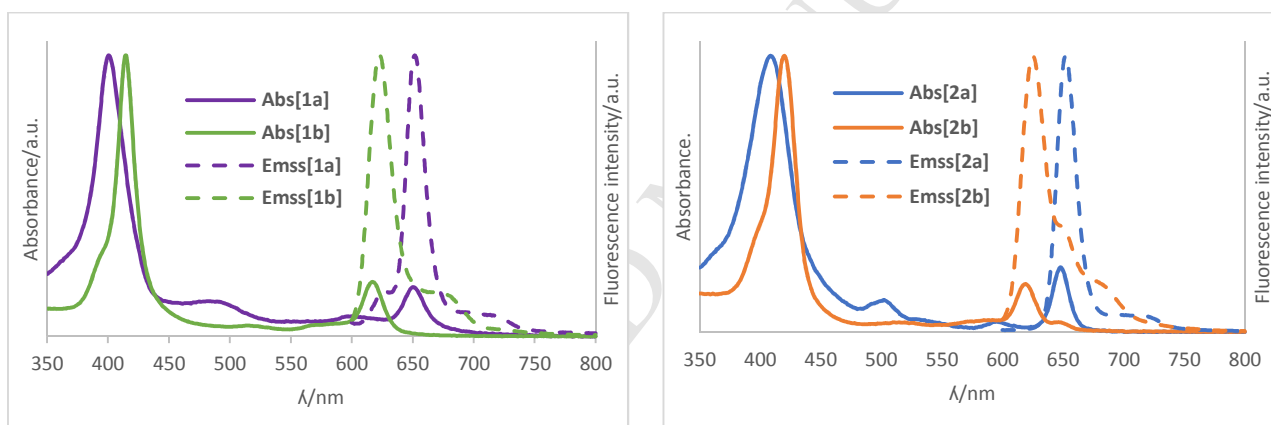
293   **Figure 1** – Normalized absorption (solid line) and emission (dashed line) spectra of compounds **1a**,**b**

294   and **2a**,**b** in DMF at 298 K.

295   The absorption spectra of Chls **1a** and **2a** (in DMF) exhibit a typical free-base Chl features with a

296   strong Soret band *ca.* 400 nm and three Q bands between 450 and 680 nm (Figure 1) being one of

297   them well defined *ca.* 650 nm. As expected, it was possible to observe changes in the absorbance

298   spectra of zinc(II)-complexed Chls **1b** and **2b** when compared with the corresponding free-bases (**1a**

299   and **2a**), having the Soret band suffered a red-shift with the disappearance of one Q band due to the

300   increase in structural symmetry, characteristic of metallochlorins.

301   The steady-state fluorescence spectra of Chls derivatives **1a**,**b** and **2a**,**b** were also achieved in DMF

302   (Figure 1) and exhibit a strong emission between 600 and 750 nm (Figure 1). The fluorescence

12

303 quantum yields (Φ_F) of the free-bases Chls **1a** and **2a** are lower than the standard porphyrin **TPP** in

304 DMF ($\Phi_F = 0.11$) [85] and Chls **1b** and **2b** are superior. It is worth to refer that the emission and the

305 fluorescence quantum yield were affected by metalation as expected [86]. The Stokes shift obtained

306 for the compounds in study were small as expected (results presented in Table 1).

307

308 **Table 1** – Photophysical properties of Chls **1a**,**b** and **2a**,**b** in DMF.

Compound	Soret (nm)	log ε	Q bands (nm)	log ε	λ_{emiss} (nm)	Stokes shift (nm)	$\Phi_F{}^a$	$\Phi_\Delta \pm 0.05^a$
1a	401	5.21	502	4.19	652	2	<0.01	0.34
			527	3.78				
			596	3.74				
			648	4.49				
1b	416	5.26	515	3.92	623	6	0.01	0.55
			585	3.98				
			618	4.56				
2a	409	4.95	503	3.53	652	4	0.07	0.39
			529	3.58				
			595	4.19				
			648	3.55				
2b	420	5.30	512	4.18	625	6	0.11	0.63
			582	3.82				
			618	4.58				
[a] Using **TPP** as reference in DMF.								

309

310 The determination of $^1O_2$ was assessed considering that it is in general the major ROS produced upon

311 irradiation by this kind of macrocycles and the main responsible for cell damage and further cell

312 death [9,15,31]. Thus, the production of $^1O_2$ by each Chl derivative was assessed by the indirect

313 method based on the absorption decay of a solution of 9,10-DMA irradiated in the presence of each

314 Chl derivatives (**1a**,**b** and **2a**,**b**) and compared with the decay in the presence of a reference (**TPP**; Φ_Δ

315 = 0.65 in DMF) (Figure SI 10). According to the results summarized in Table 1, all derivatives are

316 able to generate singlet oxygen upon light irradiation and the metallated Chls **1b** and **2b** generate

317 more singlet oxygen than the corresponding free-bases Chls **1a** and **2a**. It is worth to refer that the

318 positive charge accessibility does not affect substantially the $^1O_2$ generation.

319 Considering the potential use of these compounds as PS for PDI of *E. Coli*, the photostability of the

320 cationic Chls derivatives **1a**,**b** and **2a**,**b** was evaluated by monitoring the decrease of the absorbance

321 of their Soret, after white light irradiation at an irradiance of 25 mW.cm^{-2}, the same irradiance used

322 in the biological assays. The results are summarized in Table 2.

323

324 **Table 2** – Photostability of derivatives **1a**,**b** and **2a**,**b** in DMF after 120 min of white light irradiation

325 at an irradiance of 25 mW.cm^{-2}.

| Chl	Irradiation time (min)						
	0	**5**	**15**	**30**	**60**	**90**	**120**
1a	100	99	98	97	96	95	94
1b	100	100	100	100	100	100	100
2a	100	97	94	92	90	87	86
2b	100	100	100	100	100	100	100

326

327 Metallochlorin derivatives **1b** and **2b** show to be very photostable when irradiated with white light at

328 an irradiance of 25 mW.cm^{-2} for 120 min, meanwhile the corresponding free-bases **1a** and **2a** under

329 the same irradiation conditions show a slight decrease of the Soret band being the less stable the

14

330 chlorin **2a** with a decreased of ~15% in the Soret absorbance after 120 min of irradiation. The

331 photophysical properties exhibited by all Chls, make them suitable to be used as potential PSs and

332 allow us to assess their photodynamic efficiency against the Gram-negative bacterium *E. coli*.

Photodynamic inactivation of *Escherichia coli*

334 The PDI efficiency of cationic free-base (**1a** and **2a**) and zinc(II) (**1b** and **2b**) Chl derivatives were

335 tested against bioluminescent *E. coli*. In fact, bioluminescence has been extensively used as a real-

336 time reporter for bacterial survival/inactivation in PDI assays since the inhibition of cellular activity

337 results in a decrease in the bioluminescence rate [42,87]. In this assay a concentration of 5.0 µM was

338 used for each PS under white light irradiation at 25 mW.cm^{-2} and the results are represented in Figure

339 3.

340
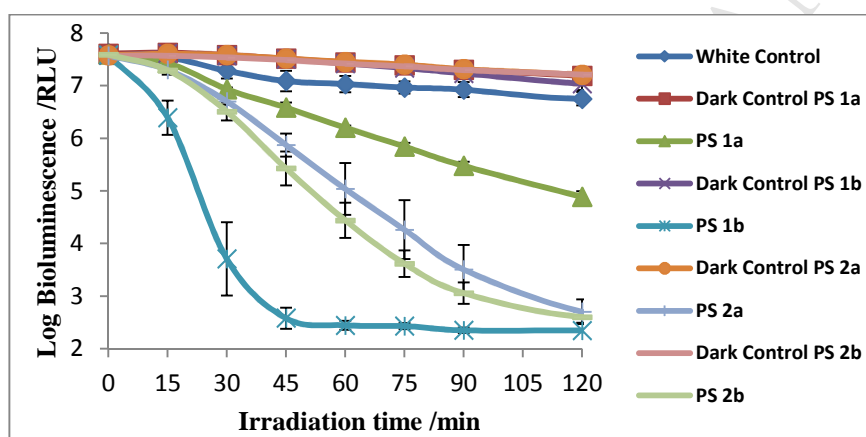
341

342 **Figure 3** – Bioluminescence monitoring of *E. coli* in the bacterial suspensions during the PDI

343 experiment in the presence of PSs **1a**,**b** and **2a**,**b** at 5.0 µM, using white light (25 mW.cm^{-2}) during

344 120 min. All values are the mean of three independent assays performed in triplicate. The error bars

345 represent the standard deviation.

346

347 None of the tested PSs showed dark toxicity (ANOVA, $p > 0.05$) since a significant decrease in

348 bioluminescence of *E. coli* was not observed during all period of irradiation. Bioluminescence of the

349 bacteria, after irradiation, in the absence of the PS also kept stable, meaning that light alone did not

350 cause any toxic effect. In the presence of each PS it was observed a significant decrease in

bioluminescence (ANOVA, $p < 0.05$) after 30 min of irradiation. The photoinactivation results obtained for the tested PSs revealed a clear difference in their photoinactivation efficiency.

It was interesting to note that the position of the charges, *N*-methylpyridinium *vs*. methoxypyridinium, influence the photodynamic inactivation efficiency of *E. coli*. That is, for the free-bases Chls (**1a** and **2a**) the most efficient compound was the one whose charge are "inverted", closer to the core (Chl **2a**). On the other hand, their zinc(II) complexed Chls (**1b** and **2b**) show higher inactivation efficiency, however the pyridinium "non-inverted" derivative, being the most effective one. These results are also interconnected with the results obtained in the $^1O_2$ production rates of each PSs, since **1b** and **2b** (metallated Chls) produce more $^1O_2$ than the corresponding free-bases **1a** and **2a**. However, a much higher PDI effect is observed between **1b** *vs*. **1a** when compared with **2b** *vs*. **2a**. The charge position did not change much the photochemical $^1O_2$ production, but at least for **1b** *vs*. **2b** this structural difference seems to be important for the photoinactivation efficacy.

Chl **1a** had already been tested against two different bacteria, *Staphylococcus aureus* (gram-(+)) and *Pseudomonas aeruginosa* (gram-(-)) [18] and at a concentration of 10.0 µM against *P. aeruginosa* showed a 7.0 log CFU.mL^{-1} reduction after 30 min of white light irradiation at an irradiance of 150 mW.cm^{-2} [18]. In the present study, using a 6-fold lower light irradiance (25 mW.cm^{-2}) and half of the PS concentration (5.0 µM), the Chl **1a** was able to reduce 2.7 log of RLU bioluminescent *E. coli* after 120 min of irradiation. More remarkable is the inactivation reached by the new metallochlorin **1b** that differs by the presence of the zinc(II) in the core. That one, after 45 min of white light irradiation, reaches the bioluminescent method detection limit (5.2 log of RLU reduction), which make it, according the guidelines of the American Society for Microbiology, a potential antibacterial agent.

A similar work assessing the antibacterial activity of a tetra- and octa-methoxypyridinium Pcs (four and eight positive charges, respectively) and the similar thiopyridinium Pcs (also four and eight charges) towards bioluminescent *E. coli* was already performed [47]. The biological results revealed that using the Pc core the inverted methoxypyridinium with eight positive charges was the most effective PS reaching 2.8 log of reduction in bioluminescence RLU after 20 min of irradiation (white

378 light, 150 mW.cm^{-2}) and at a concentration of 20.0 µM. The inverted methoxypyridinium with four

379 positive charges showed to be the less effective PS with only 0.8 log reduction in bioluminescence

380 RLU. Among the thiopyridinium Pcs, the PS with eight positive charges proved to be more effective

381 than the one with only four positive charges (2.7 and 2.3 log reductions, respectively). Once again,

382 the metallochlorin **1b** seems to be more efficient than the previous tested PS, with a bioluminescence

383 reductions of 1.2 and 3.9 log after 15 and 30 min of white light irradiation, respectively. Moreover, it

384 is important to highlight that these achievements were obtained using a four-fold lower concentration

385 (5.0 µM) and a six-fold lower irradiance (25 mW.cm^{-2}) [47], and able to generate the photochemical

386 singlet oxygen.

387

388 **Conclusions**

389 New chlorin derivatives, **1b**, **2**, **2a** and **2b**, were prepared and structurally characterized by

390 NMR spectroscopy and mass spectrometry. The photophysical characterization of the cationic

391 derivatives showed that all these Chls are photostable and able to generate singlet oxygen

392 under white light irradiation. Nevertheless, metallochlorins **1b** and **2b** are higher singlet

393 oxygen generators than the corresponding free-bases Chls **1a** and **2a**. The obtained results

394 highlight the importance of the charge position; *N*-methylpyridinium *vs*. methoxypyridinium.

395 Comparing the cationic free-bases Chls (**1a** and **2a**) the most effective PS is the Chl with

396 "inverted" pyridinium (**2a**) however for the zinc(II) complexes (**1b** and **2b**) the most effective

397 PS is *N*-methylpyridinium (**1b**).

398 The results of this study demonstrate the high PDI efficient of Chl **1b**, which achieves the

399 detection limit of the bioluminescent method (5.2 log reduction) after 45 min of white light

400 irradiation. On the other hand, methoxypyridinium Chls **2a** and **2b** possess similar

401 efficiencies (ANOVA, $p < 0.05$) and are able to reach the detection limit of the method after

402 120 min (5.2 log).

403

References

[1]   Wainwright M, Maisch T, Nonell S, Plaetzer K, Almeida A, Tegos GP, et al. Photoantimicrobials—are we afraid of the light? Lancet Infect Dis 2017;17:e49–55. doi:10.1016/S1473-3099(16)30268-7.

[2]   Magaraggia M, Faccenda F, Gandolfi A, Jori G. Treatment of microbiologically polluted aquaculture waters by a novel photochemical technique of potentially low environmental impact. J Environ Monit 2006;8:923. doi:10.1039/b606975d.

[3]   Costa L, Carvalho CMB, Faustino MAF, Neves MGPMS, Tomé JPC, Tomé AC, et al. Sewage bacteriophage inactivation by cationic porphyrins: influence of light parameters. Photochem Photobiol Sci 2010;9:1126. doi:10.1039/c0pp00051e.

[4]   Maisch T. Resistance in antimicrobial photodynamic inactivation of bacteria. Photochem Photobiol Sci 2015;14:1518–26. doi:10.1039/C5PP00037H.

429 [5] Tomé JPC, Neves MGPMS, Tomé AC, Cavaleiro JAS, Soncin M, Magaraggia M, et al.

430   Synthesis and Antibacterial Activity of New Poly- *S* -lysine–Porphyrin Conjugates. J Med

431   Chem 2004;47:6649–52. doi:10.1021/jm040802v.

432 [6] Tavares A, Carvalho CMB, Faustino MA, Neves MGPMS, Tomé JPC, Tomé AC, et al.

433   Antimicrobial Photodynamic Therapy: Study of Bacterial Recovery Viability and Potential

434   Development of Resistance after Treatment. Mar Drugs 2010;8:91–105.

435   doi:10.3390/md8010091.

436 [7] Jori G, Brown SB. Photosensitized inactivation of microorganisms. Photochem Photobiol Sci

437   2004;3:403. doi:10.1039/b311904c.

438 [8] Tünger Ö, Dinç G, Özbakkaloglu B, Atman ÜC, Algün Ü. Evaluation of rational antibiotic

439   use. Int J Antimicrob Agents 2000;15:131–5. doi:10.1016/S0924-8579(00)00158-8.

440 [9] Hamblin MR, Hasan T. Photodynamic therapy: a new antimicrobial approach to infectious

441   disease? Photochem Photobiol Sci 2004;3:436. doi:10.1039/b311900a.

442 [10] Costa L, Tomé JPC, Neves MGPMS, Tomé AC, Cavaleiro JAS, Faustino MAF, et al.

443   Evaluation of resistance development and viability recovery by a non-enveloped virus after

444   repeated cycles of aPDT. Antiviral Res 2011;91:278–82. doi:10.1016/j.antiviral.2011.06.007.

445 [11] Calin MA, Parasca S V. Light sources for photodynamic inactivation of bacteria. Lasers Med

446   Sci 2009;24:453–60. doi:10.1007/s10103-008-0588-5.

447 [12] Tavares A, Dias SRS, Carvalho CMB, Faustino MAF, Tomé JPC, Neves MGPMS, et al.

448   Mechanisms of photodynamic inactivation of a Gram-negative recombinant bioluminescent

449   bacterium by cationic porphyrins. Photochem Photobiol Sci 2011;10:1659.

450   doi:10.1039/c1pp05097d.

451 [13] Winckler KD. Special section: Focus on anti-microbial photodynamic therapy (PDT). J

452   Photochem Photobiol B Biol 2007;86:43–4. doi:10.1016/j.jphotobiol.2006.09.005.

453 [14] Caminos DA, Spesia MB, Pons P, Durantini EN. Mechanisms of Escherichia coli

454   photodynamic inactivation by an amphiphilic tricationic porphyrin and 5,10,15,20-tetra(4-

455   N,N,N-trimethylammoniumphenyl) porphyrin. Photochem Photobiol Sci 2008;7:1071.

456   doi:10.1039/b804965c.

457   [15]   Habermeyer B, Guilard R. Some activities of PorphyChem illustrated by the applications of

458   porphyrinoids in PDT, PIT and PDI. Photochem Photobiol Sci 2018;17:1675–90.

459   doi:10.1039/C8PP00222C.

460   [16]   Fu X, Fang Y, Yao M. Antimicrobial Photodynamic Therapy for Methicillin-Resistant

461   Staphylococcus aureus Infection. Biomed Res Int 2013;2013:1–9. doi:10.1155/2013/159157.

462   [17]   Nakonieczna J, Michta E, Rybicka M, Grinholc M, Gwizdek-Wiśniewska A, Bielawski KP.

463   Superoxide dismutase is upregulated in Staphylococcus aureus following protoporphyrin-

464   mediated photodynamic inactivation and does not directly influence the response to

465   photodynamic treatment. BMC Microbiol 2010;10:323. doi:10.1186/1471-2180-10-323.

466   [18]   Costa DCS, Gomes MC, Faustino MAF, Neves MGPMS, Cunha Â, Cavaleiro JAS, et al.

467   Comparative photodynamic inactivation of antibiotic resistant bacteria by first and second

468   generation cationic photosensitizers. Photochem Photobiol Sci 2012;11:1905.

469   doi:10.1039/c2pp25113b.

470   [19]   Almeida A, Faustino MA, Tomé JP. Photodynamic inactivation of bacteria: finding the

471   effective targets. Future Med Chem 2015;7:1221–4. doi:10.4155/fmc.15.59.

472   [20]   Hamblin MR, Abrahamse H. Can light-based approaches overcome antimicrobial resistance?

473   Drug Dev Res 2018:1–20. doi:10.1002/ddr.21453.

474   [21]   Zovinka EP, Sunseri DR. Photochemotherapy: Light-Dependent Therapies in Medicine. J

475   Chem Educ 2002;79:1331. doi:10.1021/ed079p1331.

476   [22]   Maisch T. A New Strategy to Destroy Antibiotic Resistant Microorganisms: Antimicrobial

477   Photodynamic Treatment. Mini-Reviews Med Chem 2009;9:974–83.

478   doi:10.2174/138955709788681582.

479 [23] Lourenço LMO, Pereira PMR, Maciel E, Válega M, Domingues FMJ, Domingues MRM, et al.

480   Amphiphilic phthalocyanine–cyclodextrin conjugates for cancer photodynamic therapy. Chem

481   Commun 2014;50:8363–6. doi:10.1039/C4CC02226B.

482 [24] Serra VV, Camões F, Vieira SI, Faustino MAF, Tomé JPC, Pinto DCGA, et al. Synthesis and

483   Biological Evaluation of Novel Chalcone-Porphyrin Conjugates. Acta Chim Slov

484   2009;56:603–11.

485 [25] Carvalho CMB, Gomes ATPC, Fernandes SCD, Prata ACB, Almeida MA, Cunha MA, et al.

486   Photoinactivation of bacteria in wastewater by porphyrins: Bacterial β-galactosidase activity

487   and leucine-uptake as methods to monitor the process. J Photochem Photobiol B Biol

488   2007;88:112–8. doi:10.1016/j.jphotobiol.2007.04.015.

489 [26] Costa L, Carvalho CMB, Tomé JPC, Faustino MAF, Neves MGPMS, Tomé AC, et al. Sewage

490   bacteriophage photoinactivation by porphyrins immobilized in solid matrixes. Curr. Res. Top.

491   Appl. Microbiol. Microb. Biotechnol., WORLD SCIENTIFIC; 2009, p. 338–41.

492   doi:10.1142/9789812837554_0071.

493 [27] Carvalho CMB, Tomé JPC, Faustino MAF, Neves MGPMS, Tomé AC, Cavaleiro JAS, et al.

494   Antimicrobial photodynamic activity of porphyrin derivatives: potential application on

495   medical and water disinfection. J Porphyr Phthalocyanines 2009;13:574–7.

496   doi:10.1142/S1088424609000528.

497 [28] Plaetzer K, Berneburg M, Kiesslich T, Maisch T. New Applications of Photodynamic Therapy

498   in Biomedicine and Biotechnology. Biomed Res Int 2013;2013:1–3.

499   doi:10.1155/2013/161362.

500 [29] Bhupathiraju NVSDK, Rizvi W, Batteas JD, Drain CM. Fluorinated porphyrinoids as efficient

501   platforms for new photonic materials, sensors, and therapeutics. Org Biomol Chem

502   2016;14:389–408. doi:10.1039/C5OB01839K.

503 [30] Cassidy CM, Tunney MM, McCarron PA, Donnelly RF. Drug delivery strategies for

504 photodynamic antimicrobial chemotherapy: From benchtop to clinical practice. J Photochem

505 Photobiol B Biol 2009;95:71–80. doi:10.1016/j.jphotobiol.2009.01.005.

506 [31] Maisch T. Anti-microbial photodynamic therapy: useful in the future? Lasers Med Sci

507 2007;22:83–91. doi:10.1007/s10103-006-0409-7.

508 [32] Mesquita MQ, Menezes JCJMDS, Pires SMG, Neves MGPMS, Simões MMQ, Tomé AC, et

509 al. Pyrrolidine-fused chlorin photosensitizer immobilized on solid supports for the

510 photoinactivation of Gram negative bacteria. Dye Pigment 2014;110:123–33.

511 doi:10.1016/j.dyepig.2014.04.025.

512 [33] Marciel L, Teles L, Moreira B, Pacheco M, Lourenço LM, Neves MG, et al. An effective and

513 potentially safe blood disinfection protocol using tetrapyrrolic photosensitizers. Future Med

514 Chem 2017;9:365–79. doi:10.4155/fmc-2016-0217.

515 [34] Lourenço LMO, Iglesias BA, Pereira PMR, Girão H, Fernandes R, Neves MGPMS, et al.

516 Synthesis, characterization and biomolecule-binding properties of novel tetra-platinum(II)-

517 thiopyridylporphyrins. Dalt Trans 2015;44:530–8. doi:10.1039/C4DT02697G.

518 [35] Moura NMM, Ramos CI V., Linhares I, Santos SM, Faustino MAF, Almeida A, et al.

519 Synthesis, characterization and biological evaluation of cationic porphyrin–terpyridine

520 derivatives. RSC Adv 2016;6:110674–85. doi:10.1039/C6RA25373C.

521 [36] Moura NMM, Esteves M, Vieira C, Rocha GMSRO, Faustino MAF, Almeida A, et al. Novel

522 β-functionalized mono-charged porphyrinic derivatives: Synthesis and photoinactivation of

523 Escherichia coli. Dye Pigment 2019;160:361–71. doi:10.1016/j.dyepig.2018.06.048.

524 [37] Q. Mesquita M, J. Dias C, P. M. S. Neves M, Almeida A, F. Faustino M. Revisiting Current

525 Photoactive Materials for Antimicrobial Photodynamic Therapy. Molecules 2018;23:2424.

526 doi:10.3390/molecules23102424.

527 [38] Amin RM, Bhayana B, Hamblin MR, Dai T. Antimicrobial blue light inactivation of

528 Pseudomonas aeruginosa by photo-excitation of endogenous porphyrins: In vitro and in vivo

529   studies. Lasers Surg Med 2016;48:562–8. doi:10.1002/lsm.22474.

530   [39]   Huang L, El-Hussein A, Xuan W, Hamblin MR. Potentiation by potassium iodide reveals that

531   the anionic porphyrin TPPS4 is a surprisingly effective photosensitizer for antimicrobial

532   photodynamic inactivation. J Photochem Photobiol B Biol 2018;178:277–86.

533   doi:10.1016/j.jphotobiol.2017.10.036.

534   [40]   Faraj Tabrizi P, Wennige S, Berneburg M, Maisch T. Susceptibility of sodA- and sodB-

535   deficient Escherichia coli mutant towards antimicrobial photodynamic inactivation via the type

536   I-mechanism of action. Photochem Photobiol Sci 2018;17:352–62. doi:10.1039/C7PP00370F.

537   [41]   Felgenträger A, Maisch T, Späth A, Schröder JA, Bäumler W. Singlet oxygen generation in

538   porphyrin-doped polymeric surface coating enables antimicrobial effects on Staphylococcus

539   aureus. Phys Chem Chem Phys 2014;16:20598–607. doi:10.1039/C4CP02439G.

540   [42]   Mesquita MQ, Menezes JCJMDS, Neves MGPMS, Tomé AC, Cavaleiro JAS, Cunha Â, et al.

541   Photodynamic inactivation of bioluminescent Escherichia coli by neutral and cationic

542   pyrrolidine-fused chlorins and isobacteriochlorins. Bioorg Med Chem Lett 2014;24:808–12.

543   doi:10.1016/j.bmcl.2013.12.097.

544   [43]   Singh S, Aggarwal A, Thompson S, Tomé JPC, Zhu X, Samaroo D, et al. Synthesis and

545   Photophysical Properties of Thioglycosylated Chlorins, Isobacteriochlorins, and

546   Bacteriochlorins for Bioimaging and Diagnostics. Bioconjug Chem 2010;21:2136–46.

547   doi:10.1021/bc100356z.

548   [44]   GOMES ATPC, NEVES MGPMS, CAVALEIRO JAS. Cancer, Photodynamic Therapy and

549   Porphyrin-Type Derivatives. An Acad Bras Cienc 2018;90:993–1026. doi:10.1590/0001-

550   3765201820170811.

551   [45]   Yang E, Diers JR, Huang Y-Y, Hamblin MR, Lindsey JS, Bocian DF, et al. Molecular

552   Electronic Tuning of Photosensitizers to Enhance Photodynamic Therapy: Synthetic

553   Dicyanobacteriochlorins as a Case Study. Photochem Photobiol 2013;89:605–18.

554   doi:10.1111/php.12021.

555   [46]   Huang L, Wang M, Huang Y-Y, El-Hussein A, Wolf LM, Chiang LY, et al. Progressive

556   cationic functionalization of chlorin derivatives for antimicrobial photodynamic inactivation

557   and related vancomycin conjugates. Photochem Photobiol Sci 2018;17:638–51.

558   doi:10.1039/C7PP00389G.

559   [47]   Lourenço LMO, Sousa A, Gomes MC, Faustino MAF, Almeida A, Silva AMS, et al. Inverted

560   methoxypyridinium phthalocyanines for PDI of pathogenic bacteria. Photochem Photobiol Sci

561   2015;14:1853–63. doi:10.1039/C5PP00145E.

562   [48]   Lourenço LMO, Neves MGPMS, Cavaleiro JAS, Tomé JPC. Synthetic approaches to

563   glycophthalocyanines. Tetrahedron 2014;70:2681–98. doi:10.1016/j.tet.2014.01.058.

564   [49]   Spesia MB, Rovera M, Durantini EN. Photodynamic inactivation of Escherichia coli and

565   Streptococcus mitis by cationic zinc(II) phthalocyanines in media with blood derivatives. Eur J

566   Med Chem 2010;45:2198–205. doi:10.1016/j.ejmech.2010.01.058.

567   [50]   Junqueira JC, Jorge AOC, Barbosa JO, Rossoni RD, Vilela SFG, Costa ACBP, et al.

568   Photodynamic inactivation of biofilms formed by Candida spp., Trichosporon mucoides, and

569   Kodamaea ohmeri by cationic nanoemulsion of zinc 2,9,16,23-tetrakis(phenylthio)-29H, 31H-

570   phthalocyanine (ZnPc). Lasers Med Sci 2012;27:1205–12. doi:10.1007/s10103-012-1050-2.

571   [51]   Spesia MB, Caminos DA, Pons P, Durantini EN. Mechanistic insight of the photodynamic

572   inactivation of Escherichia coli by a tetracationic zinc(II) phthalocyanine derivative.

573   Photodiagnosis Photodyn Ther 2009;6:52–61. doi:10.1016/j.pdpdt.2009.01.003.

574   [52]   Ke M-R, Eastel JM, Ngai KLK, Cheung Y-Y, Chan PKS, Hui M, et al. Photodynamic

575   inactivation of bacteria and viruses using two monosubstituted zinc(II) phthalocyanines. Eur J

576   Med Chem 2014;84:278–83. doi:10.1016/j.ejmech.2014.07.022.

577   [53]   Lourenço LMO, Rocha DMGC, Ramos CI V., Gomes MC, Almeida A, Faustino MAF, et al.

578   Photoinactivation of Planktonic and Biofilm Forms of Escherichia coli Through the Action of

579   Cationic Zinc(II) Phthalocyanines. ChemPhotoChem 2019. doi:10.1002/cptc.201900020.

580 [54] Hao E, Friso E, Miotto G, Jori G, Soncin M, Fabris C, et al. Synthesis and biological

581   investigations of tetrakis(p-carboranylthio-tetrafluorophenyl)chlorin (TPFC). Org Biomol

582   Chem 2008;6:3732–40. doi:10.1039/b807836j.

583 [55] Yano S, Hirohara S, Obata M, Hagiya Y, Ogura S, Ikeda A, et al. Current states and future

584   views in photodynamic therapy. J Photochem Photobiol C Photochem Rev 2011;12:46–67.

585   doi:10.1016/j.jphotochemrev.2011.06.001.

586 [56] Singh S, Aggarwal A, Bhupathiraju NVSDK, Arianna G, Tiwari K, Drain CM. Glycosylated

587   Porphyrins, Phthalocyanines, and Other Porphyrinoids for Diagnostics and Therapeutics.

588   Chem Rev 2015;115:10261–306. doi:10.1021/acs.chemrev.5b00244.

589 [57] SCHEER H, INHOFFEN HH. Hydroporphyrins: Reactivity, Spectroscopy, and

590   Hydroporphyrin Analogues. The Porphyrins, Elsevier; 1978, p. 45–90. doi:10.1016/B978-0-

591   12-220102-8.50009-9.

592 [58] Alves E, Faustino MAF, Neves MGPMS, Cunha Â, Nadais H, Almeida A. Potential

593   applications of porphyrins in photodynamic inactivation beyond the medical scope. J

594   Photochem Photobiol C Photochem Rev 2015;22:34–57.

595   doi:10.1016/j.jphotochemrev.2014.09.003.

596 [59] Yin R, Agrawal T, Khan U, Gupta GK, Rai V, Huang Y-Y, et al. Antimicrobial photodynamic

597   inactivation in nanomedicine: small light strides against bad bugs. Nanomedicine

598   2015;10:2379–404. doi:10.2217/nnm.15.67.

599 [60] Bartolomeu M, Reis S, Fontes M, Neves M, Faustino M, Almeida A. Photodynamic Action

600   against Wastewater Microorganisms and Chemical Pollutants: An Effective Approach with

601   Low Environmental Impact. Water 2017;9:630. doi:10.3390/w9090630.

602 [61] Silva AF, Borges A, Giaouris E, Graton Mikcha JM, Simões M. Photodynamic inactivation as

603   an emergent strategy against foodborne pathogenic bacteria in planktonic and sessile states.

604 Crit Rev Microbiol 2018;0:1–18. doi:10.1080/1040841X.2018.1491528.

605 [62] Hirohara S, Obata M, Alitomo H, Sharyo K, Ando T, Tanihara M, et al. Synthesis,

606 photophysical properties and sugar-dependent in vitro photocytotoxicity of pyrrolidine-fused

607 chlorins bearing S-glycosides. J Photochem Photobiol B Biol 2009;97:22–33.

608 doi:10.1016/j.jphotobiol.2009.07.007.

609 [63] Aggarwal A, Thompson S, Singh S, Newton B, Moore A, Gao R, et al. Photophysics of

610 Glycosylated Derivatives of a Chlorin, Isobacteriochlorin and Bacteriochlorin for

611 Photodynamic Theragnostics: Discovery of a Two-photon-absorbing Photosensitizer.

612 Photochem Photobiol 2014;90:419–30. doi:10.1111/php.12179.

613 [64] DeRosa M. Photosensitized singlet oxygen and its applications. Coord Chem Rev 2002;233–

614 234:351–71. doi:10.1016/S0010-8545(02)00034-6.

615 [65] Pereira NAM, Laranjo M, Casalta-Lopes J, Serra AC, Piñeiro M, Pina J, et al. Platinum(II)

616 Ring-Fused Chlorins as Near-Infrared Emitting Oxygen Sensors and Photodynamic Agents.

617 ACS Med Chem Lett 2017;8:310–5. doi:10.1021/acsmedchemlett.6b00476.

618 [66] Bonnett R, Buckley DG, Burrow T, Galia ABB, Saville B, Songca SP. Photobactericidal

619 materials based on porphyrins and phthalocyanines. J Mater Chem 1993;3:323.

620 doi:10.1039/jm9930300323.

621 [67] Nazzal S, Chen C-P, Tsai T. Nanotechnology in Antimicrobial Photodynamic Inactivation. J

622 Food Drug Anal 2011;19:383–95.

623 [68] Hamblin MR, O´Donnell DA, Murthy N, Rajagopalan K, Michaud N, Sherwood ME, et al.

624 Polycationic photosensitizer conjugates: effects of chain length and Gram classification on the

625 photodynamic inactivation of bacteria. J Antimicrob Chemother 2002;49:941–51.

626 doi:10.1093/jac/dkf053.

627 [69] Polo L, Segalla A, Bertoloni G, Jori G, Schaffner K, Reddi E. Polylysine–porphycene

628 conjugates as efficient photosensitizers for the inactivation of microbial pathogens. J

Photochem Photobiol B Biol 2000;59:152–8. doi:10.1016/S1011-1344(01)00114-2.

[70]   Alves E, Faustino MAF, Neves MGPMS, Cunha A, Tome J, Almeida A. An insight on bacterial cellular targets of photodynamic inactivation. Future Med Chem 2014;6:141–64. doi:10.4155/fmc.13.211.

[71]   Pereira MA, Faustino MAF, Tomé JPC, Neves MGPMS, Tomé AC, Cavaleiro JAS, et al. Influence of external bacterial structures on the efficiency of photodynamic inactivation by a cationic porphyrin. Photochem Photobiol Sci 2014;13:680. doi:10.1039/c3pp50408e.

[72]   Alves E, Costa L, Carvalho CM, Tomé JP, Faustino MA, Neves MG, et al. Charge effect on the photoinactivation of Gram-negative and Gram-positive bacteria by cationic meso-substituted porphyrins. BMC Microbiol 2009;9:70. doi:10.1186/1471-2180-9-70.

[73]   Simões C, Gomes MC, Neves MGPMS, Cunha Â, Tomé JPC, Tomé AC, et al. Photodynamic inactivation of Escherichia coli with cationic meso -tetraarylporphyrins – The charge number and charge distribution effects. Catal Today 2016;266:197–204. doi:10.1016/j.cattod.2015.07.031.

[74]   Marciel L, Mesquita MQ, Ferreira R, Moreira B, Neves MGPMS, Faustino MAF, et al. An efficient formulation based on cationic porphyrins to photoinactivate Staphylococcus aureus and Escherichia coli. Future Med Chem 2018;10:1821–33. doi:10.4155/fmc-2018-0010.

[75]   Almeida J, Tomé JPC, Neves MGPMS, Tomé AC, Cavaleiro JAS, Cunha Â, et al. Photodynamic inactivation of multidrug-resistant bacteria in hospital wastewaters: influence of residual antibiotics. Photochem Photobiol Sci 2014;13:626. doi:10.1039/c3pp50195g.

[76]   Armarego WLF, Chai CLL. Purification of Organic Chemicals. Purif. Lab. Chem., Elsevier; 2009. doi:10.1016/B978-1-85617-567-8.50012-3.

[77]   Gomes A, Fernandes E, Lima JLFC. Fluorescence probes used for detection of reactive oxygen species. J Biochem Biophys Methods 2005;65:45–80. doi:10.1016/j.jbbm.2005.10.003.

654 [78] Castro-Olivares R, Günther G, Zanocco AL, Lemp E. Linear free energy relationship analysis

655 of solvent effect on singlet oxygen reactions with mono and disubstituted anthracene

656 derivatives. J Photochem Photobiol A Chem 2009;207:160–6.

657 doi:10.1016/j.jphotochem.2009.05.012.

658 [79] Menezes JCJMDS, Faustino MAF, de Oliveira KT, Uliana MP, Ferreira VF, Hackbarth S, et

659 al. Synthesis of New Chlorin e 6 Trimethyl and Protoporphyrin IX Dimethyl Ester Derivatives

660 and Their Photophysical and Electrochemical Characterizations. Chem - A Eur J

661 2014;20:13644–55. doi:10.1002/chem.201403214.

662 [80] Alves E, Costa L, Cunha Â, Faustino MAF, Neves MGPMS, Almeida A. Bioluminescence

663 and its application in the monitoring of antimicrobial photodynamic therapy. Appl Microbiol

664 Biotechnol 2011;92:1115–28. doi:10.1007/s00253-011-3639-y.

665 [81] Costa L, Alves E, Carvalho CMB, Tomé JPC, Faustino MAF, Neves MGPMS, et al. Sewage

666 bacteriophage photoinactivation by cationic porphyrins: a study of charge effect. Photochem

667 Photobiol Sci 2008;7:415. doi:10.1039/b712749a.

668 [82] Costa DCS, Pais VF, Silva AMS, Cavaleiro JAS, Pischel U, Tomé JPC. Cationic porphyrins

669 with inverted pyridinium groups and their fluorescence properties. Tetrahedron Lett

670 2014;55:4156–9. doi:10.1016/j.tetlet.2014.05.108.

671 [83] Ramos CI V., Marques MGS, Correia AJF, Serra VV, Tomé JPC, Tomé AC, et al. Reduction

672 of cationic free-base meso-tris-N-methylpyridinium-4-yl porphyrins in positive mode

673 electrospray ionization mass spectrometry. J Am Soc Mass Spectrom 2007;18:762–8.

674 doi:10.1016/j.jasms.2006.12.009.

675 [84] Ramos CI V., Santana-Marques MG, Ferrer Correia AJ, Tomé JPC, Alonso CM, Tomé AC, et

676 al. Reduction and adduct formation from electrosprayed solutions of porphyrin salts. J Mass

677 Spectrom 2008;43:806–13. doi:10.1002/jms.1378.

678 [85] Silva S, Pereira PMR, Silva P, Almeida Paz FA, Faustino MAF, Cavaleiro JAS, et al.

679   Porphyrin and phthalocyanine glycodendritic conjugates: synthesis, photophysical and

680   photochemical properties. Chem Commun 2012;48:3608. doi:10.1039/c2cc17561d.

681   [86] Moura NMM, Faustino MAF, Neves MGPMS, Tomé AC, Rakib EM, Hannioui A, et al. Novel

682   pyrazoline and pyrazole porphyrin derivatives: synthesis and photophysical properties.

683   Tetrahedron 2012;68:8181–93. doi:10.1016/j.tet.2012.07.072.

684   [87] Alves E, Carvalho CMB, Tomé JPC, Faustino MAF, Neves MGPMS, Tomé AC, et al.

685   Photodynamic inactivation of recombinant bioluminescent Escherichia coli by cationic

686   porphyrins under artificial and solar irradiation. J Ind Microbiol Biotechnol 2008;35:1447–54.

687   doi:10.1007/s10295-008-0446-2.

688

Highlights

•

PDI with pyridinium or inverted pyridinium chlorin derivatives was effective to inactivate *Escherichia coli*.

•

Chlorins are photostable and able to generate singlet oxygen under white light irradiation.

•

The charge position *N*-methylpyridinium vs. methoxypyridinium influences the PDI effect.

•

High PDI efficiency of chlorin **1b**, which achieves the detection limit of the bioluminescent method (5.2 log reduction) after 45 min of white light irradiation.